Wavelet analysis of corneal endothelial electrical potential difference reveals cyclic operation of the secretory mechanism

V. I. Cacace,[1] N. Montalbetti,[1] C. Kusnier,[1] M. P. Gomez,[2] and J. Fischbarg[1,*]

[1]*Institute of Cardiological Investigations, University of Buenos Aires, Buenos Aires, Argentina 1122 and CONICET, Buenos Aires, Argentina*

[2]*National Commission of Atomic Energy, Group of Elastic Waves, National Commission of Atomic Energy, Buenos Aires, Argentina 1650 and Acoustic Emission Group, National Technological University, Campana, Argentina 2804*

(Received 15 June 2011; revised manuscript received 1 August 2011; published 19 September 2011)

The corneal endothelium is a fluid-transporting epithelium. As other similar tissues, it displays an electrical potential of ∼1 mV (aqueous side negative) across the entire layer [transendothelial potential difference (TEPD)]. It appears that this electrical potential is mainly the result of the transport of anions across the cell layer (from stroma to aqueous). There is substantial evidence that the TEPD is related linearly to fluid transport; hence, under proper conditions, its measure could serve as a measure of fluid transport. Furthermore, the TEPD is not steady; instead, it displays a spectrum of frequency components (0–15 Hz) recognized recently using Fourier transforms. Such frequency components appear due to charge-separating (electrogenic) processes mediated by epithelial plasma membrane proteins (both ionic channels and ionic cotransporters). In particular, the endothelial TEPD oscillations of the highest amplitude (1–2 Hz) were linked to the operation of so-called sodium bicarbonate cotransporters. However, no time localization of that activity could be obtained with the Fourier methodology utilized. For that reason we now characterize the TEPD using wavelet analysis with the aim to localize in time the variations in TEPD. We find that the mentioned high-amplitude oscillatory components of the TEPD appear cyclically during the several hours that an endothelial preparation survives *in vitro*. They have a period of 4.6 ± 0.4 s on average (n=4). The wavelet power value at the peak of such oscillations is 1.5 ± 0.1 mV^2 Hz on average ($n = 4$), and is remarkably narrow in its distribution.

DOI: 10.1103/PhysRevE.84.032902 PACS number(s): 87.18.Nq, 87.10.−e

I. INTRODUCTION

The posterior epithelium of the cornea, commonly known as "corneal endothelium," is a monocellular layer which transports fluid from the corneal stroma into the aqueous chamber. Since the corneal stroma tends naturally to imbibe water and become opaque, this fluid transfer keeps the stroma somewhat dehydrated, which optimizes the milieu to preserve corneal transparency [1].

As other fluid transporting epithelia, the corneal endothelium generates a transendothelial electrical potential difference (TEPD) across the entire cell layer (between the stroma or basolateral side, and the aqueous, or apical side; ∼1 mV, aqueous negative). From such orientation, the TEPD would arise in good part from the active transport of anions through the cell layer. Moreover, the TEPD gives rise to a local electrical current that circulates around the cells; net current across the tissue is zero.

There is evidence that this TEPD is linearly related to the magnitude of the fluid secretion [2,3]. Hence, determination of the TEPD would serve as a measure of the fluid movement.

The corneal endothelial TEPD has been recognized recently to be characteristically noisy; in fact, it displays a spectrum of oscillatory components of frequencies between 0 and 15 Hz [4]. In that paper, we use the Fourier transform to analyze the TEPD. In particular, the high-amplitude, low-frequency oscillations shown in that spectrum were linked to the operation of charge-separating ("electrogenic") plasma membrane proteins, specifically the so-called sodium bicarbonate cotransporters. These proteins transport either two or three bicarbonate ions and one sodium ion in each cycle of operation, therefore separating the charge. However, no time localization of that activity could be resolved with the Fourier methodology utilized.

For that reason we now characterize the TEPD using wavelet analysis with the aim to localize in time the variations in TEPD. The main difference between these two methods is that the standard Fourier transform is only localized in frequency, whereas wavelets are localized in both frequency and time. We find that the high-amplitude, low-frequency oscillations of the TEPD take place throughout the experiment, with a mean period of 4.6 ± 0.4 s ($n = 4$). The wavelet power value at the peak of such oscillations is 1.5 ± 0.1 mV^2 Hz in the average ($n = 4$), and is remarkably narrow in its distribution.

II. MATERIALS AND METHODS

A. Endothelial dissection and mounting

Experiments were done using *in vitro* rabbit corneal endothelial preparations. Techniques for the recording of the electrical potential difference across it have been described previously [5,6]. Corneas were obtained from New Zealand albino rabbits (∼2 kg) using procedures complying with institutional and national guidelines for the use and care of laboratory animals. Rabbits were euthanized by injecting a sodium pentobarbital solution into the marginal ear vein. The eyes were enucleated immediately. The cornea was deepithelialized and dissected using the method of Dikstein and Maurice [7], and was mounted in a jacketed Ussing

*Corresponding author. Jorge Fischbarg, M.D., Ph.D., Institute of Cardiological Investigations "A.C. Taquini" (ININCA-UBA-CONICET), Marcelo T. de Alvear 2270, C1122AAJ Buenos Aires, Argentina. Email: fischbargj@fmed.uba.ar

chamber ($T = 37$ C). Both endothelial surfaces (aqueous and stromal) were bathed with an air-bubbled HEPES-HCO_3^- solution containing (in mmol/liter) 104.4 NaCl, 26.2 $NaHCO_3$, 3.8 KCl, 1 NaH_2PO_4, 0.78 $MgSO_4$, 1.7 $CaCl_2$, 6.9 glucose, and 20 HEPES Na. The cornea was supported by a hemispherical stainless steel net, and subject to a hydrostatic pressure difference of 3 cm H_2O applied to the aqueous (endothelial) side.

B. Measurements of transendothelial electrical potential difference

The TEPD was determined with a differential electrometer amplifier (Model 604; Keithley Instruments, Inc., Cleveland, OH) connected to calomel electrodes and salt bridges. Small electrical asymmetries between electrodes were nullified with an adjustable series battery. The TEPD (typically 0.5–1.5 mV) was amplified by the electrometer by 10^3 and sent through a filter (HI/LO 1020F; Rockland Labs, Tappan, NY; low pass cutoff=10 KHz). This processed signal was displayed on an oscilloscope, digitized at 500 Hz with a data acquisition system for electrophysiology recordings (Digidata 1440A, Axon Instruments, Forest City, CA), and stored in a PC with the help of the program PCLAMP (Axon Instruments). Each experiment was done in a different corneal preparation.

C. Transendothelial electrical potential difference temporal records analysis

1. Wavelet transform

The wavelet transform (W) is a time-scale (or time-frequency) transformation of continuous or discrete signals, and is more general than the windowed Fourier transform. It allows a multiresolution analysis of the signal in the time-scale field, showing good resolution in time for high frequencies and good resolution in frequency for low frequencies [8,9].

The normalized wavelet function is defined as

$$\Psi_{a,b}(t) = \frac{1}{\sqrt{|a|}}\Psi\left(\frac{t-b}{a}\right), \tag{1}$$

where $\Psi(t)$ is the mother wavelet function, and a and b are dilation and location parameters.

There are some requirements to consider a function as a wavelet. It must have finite energy, a mean value of zero, and for complex wavelets, the Fourier transform must be real, and must vanish for negative frequencies.

The continuous W of a continuous signal $f(t)$ is defined as

$$\mathcal{W}(a,b) = \int_{-\infty}^{\infty} f(t)\Psi^*_{a,b}(t)dt,$$

where $\Psi^*_{a,b}$ is the complex conjugate of the function $\Psi_{a,b}$.

A discretization of the transform integrals can be performed to solve the continuous W of a discretized signal $f(t)$, replacing the continuous integral by a discrete summation in time, with discrete evolution of parameters a and b where $t{=}n_t\Delta t$ and $b = n_b\Delta t$:

$$\mathcal{W}(a,n_b) = \frac{1}{\sqrt{a}}\sum_{n_t=0}^{N-1} f(n_t\Delta t)\Psi^*_{a,b}\left[\frac{(n_t-n_b)}{a}\Delta t\right],$$

with $n_b = 0\cdots N-1$.

Another form to show the wavelet transform is by means of the convolution in time between the measured signal and the mother wavelet:

$$\mathcal{W}(a,b) = f(t)\otimes\Psi^*_{a,b}(t).$$

Using the convolution theorem [10], the wavelet transform can be expressed as

$$\mathcal{W}(a) = \mathcal{I}\left\{\frac{1}{\sqrt{a}}\mathcal{F}[f(n,\Delta t)]\mathcal{F}[\Psi(n,\Delta t,a)]\right\}.$$

The benefit of the latest expression is the computational speed of resolution using the fast Fourier transform $\mathcal{F}$ and the inverse fast Fourier transform $\mathcal{I}$. The aim of these equations is to find the wavelet coefficients (or amplitudes) as a function of time and scale (which is related to frequency). The wavelet power spectrum is defined as the absolute value squared of the wavelet coefficients.

D. Analysis of the TEPD records

Wavelet analysis of TEPD was done using two routines written in MATLAB. The first routine operated on the temporal record of the TEPD, and yielded the amplitudes of all frequencies up to 15 Hz. In this work, the Morlet function was selected as the mother wavelet. To concentrate on the analysis of the frequencies of most interest, a second routine was developed that considered only the frequencies between 0.5 and 2 Hz. It averaged the squared absolute values of the amplitudes (wavelet power) in the frequency domain, and gave as output a table of the times and the averaged wavelet power.

We subsequently took the temporal sequence of the wavelet power, and ran the ORIGIN (OriginLab Corp., Northampton, MA) pick peaks routine, with parameters of width 5%, height 5%, and minimum height 5%, thus determining the time and amplitude of the peaks for a given experiment. We then constructed two histograms: (1) for the time differences between the peaks (in s), and (2) for their wavelet powers (in V^2 Hz). We obtained fits for them using ORIGIN lognormal distribution. Results are expressed as mean±standard error (SE).

III. RESULTS

A. Temporal records of TEPD and wavelet analysis

We obtained temporal records of the electrical potential difference between the two experimental hemichambers filled with saline, with ($n = 4$) and without ($n = 3$) corneal preparations mounted in between them. As was reported earlier [4], a characteristic behavior of temporal records of the TEPD was observed only with preparations present (Fig. 1 top panel). By comparison, controls with only solution in the chambers were remarkably flat. Subsequently, we performed a wavelet analysis of the temporal record of the TEPD and we obtained a three-dimensional (3D) graph (Fig. 1) depicting the frequency (on the ordinate), the time (on the abscissa), and in the z axis (towards the observer), the amplitude color coded with red being high amplitude (blue is background; Fig. 1 bottom panel).

Inspection of these figures revealed most often a periodicity; as Fig. 1 shows, low-frequency amplitudes were present in packets or groups occurring every ∼4–5 s. Based on this

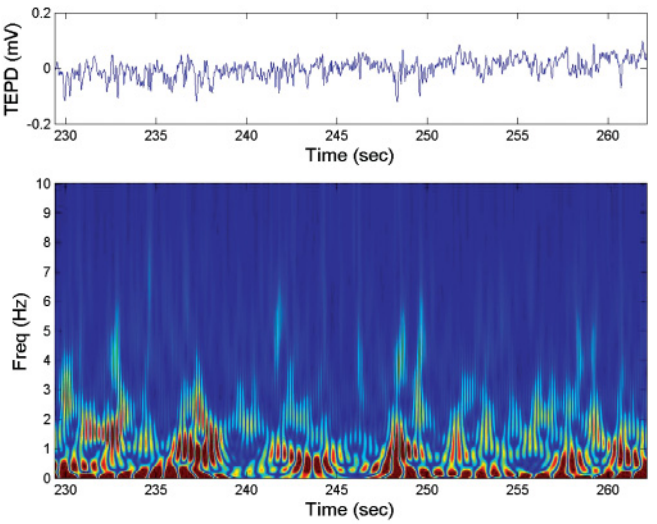

FIG. 1. (Color) Wavelet analysis of the temporal record of TEPD (representative experiment). Top panel: transendothelial electrical potential difference (in mV) as a function of time. As time increases, the TEPD goes down gradually as the preparation decays. Bottom panel: 3D graph depicting on the ordinate, the frequency; on the abscissa, the time; on the z axis (towards the observer), the amplitude color coded with red being high amplitude and the blue denoting the background. The bottom panel was obtained from the data in the top panel, treated with the wavelet-decomposition routine run in MATLAB.

qualitative perception, we devised the analytical procedure that follows.

B. Analysis of the wavelet power of the TEPD

We limit our analysis to the low frequencies of most interest (0.5–2 Hz), and we determine the time and the wavelet power

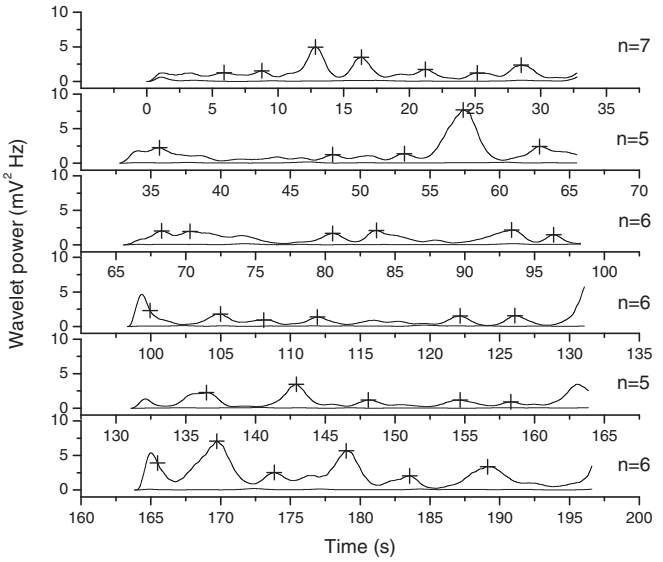

FIG. 2. Representative experiment of wavelet power. Of all the data (between 0 and 15 Hz), the MATLAB routine selected only the region of highest wavelet power (between 0.5 and 2 Hz), squared them, and averaged them. The resulting wavelet power is plotted against time for the first 197 s. The crosses denote the times at which peaks were found using ORIGIN; n is the number of peaks in each row.

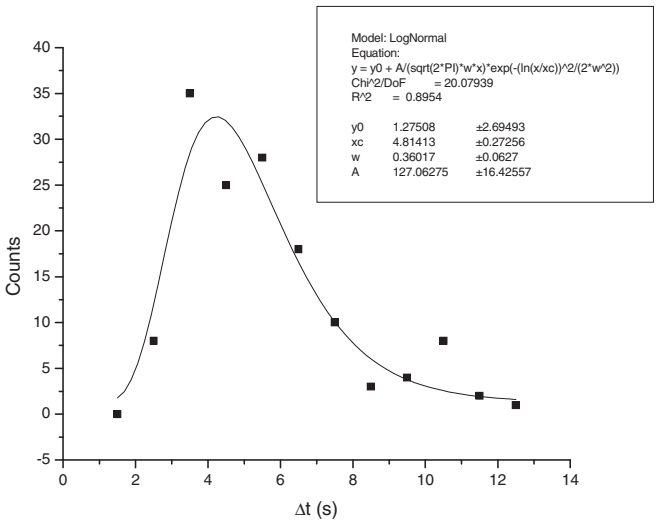

FIG. 3. The time intervals between peaks for experiment 1 in Fig. 2 (Δt's) are grouped in a histogram. A fit to the lognormal distribution (done in ORIGIN) yields an average time interval of 4.8 ± 0.3 s.

peaks for each experiment. For convenience, only the first 195 s of an experiment are shown in Fig. 2. In the time domain, the peaks correspond to periods of ∼5 s (Fig. 2). In contrast, only a flat base line with negligible noise was obtained in control experiments generated by the solution-filled chamber, which rules out possible artifacts from electrodes, electrometer, or unspecified sources (data not shown).

To quantify these results we obtained the histograms for the time differences between peaks (Δt), and for their wavelet powers. Figure 3 shows the histogram for the Δt's obtained from the data shown in Fig. 2. A fit to the lognormal distribution yields for that particular experiment a time interval of 4.8 ± 0.3 s (0.21 Hz). The wavelet power peak amplitudes of Fig. 2

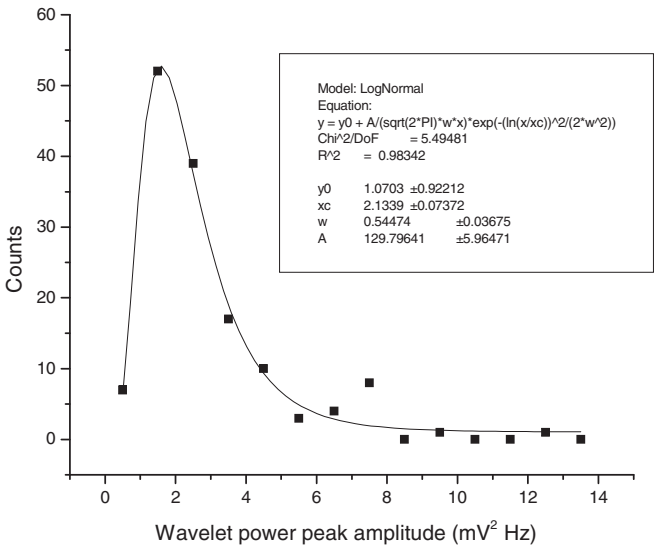

FIG. 4. The wavelet power peak amplitudes of Fig. 2 are grouped into a histogram and fitted to the lognormal distribution by ORIGIN. The average value is 2.1 ± 0.1 mV^2 Hz; note the relative narrowness of the distribution.

TABLE I. Summary of wavelet power peak amplitudes, and Δt's of all experiments.

Experiment	Wavelet power (mV^2 Hz)	Δt (s)
1	2.13 ± 0.07	4.81 ± 0.27
2	1.48 ± 0.08	4.38 ± 0.26
3	0.95 ± 0.03	4.69 ± 0.09
4	1.56 ± 0.05	4.54 ± 0.18
Mean $\pm$ SE	1.53 ± 0.12	4.59 ± 0.43

were in turn grouped into a histogram and fitted again to the lognormal distribution (Fig. 4), which yielded for that experiment an amplitude of 2.1 ± 0.1 mV^2 Hz. A summary of the values for Δt and wavelet power peak amplitudes for all four experiments is given in Table I.

IV. DISCUSSION

The oscillatory nature of the TEPD recognized recently was achieved with Fourier analysis. What that methodology could not resolve was when in time did the oscillations appear during the experiment. This limitation is now circumvented by the use of wavelet analysis. The most important conclusion is that the high-amplitude oscillations of the TEPD occur all throughout the experiment, without significant calm or rest periods, repeating themselves with a period of (Table I) 4.6 ± 0.4 s (0.22 Hz). The wavelet power at the peak of such oscillations is 1.5 ± 0.1 mV^2 Hz (Table I) on average, and is remarkably narrow in its distribution.

Low-frequency activity in the TEPD was attributed to the functioning of sodium bicarbonate cotransporters in a recent publication of ours [4] which analyzed the power spectrum of the TEPD. The current observations with wavelet analysis confirm and extend the prior findings; the low-frequency oscillations of the TEPD, attributable to sodium bicarbonate cotransport, occur in the fashion just described.

Enzymes, transporter proteins, and cotransporter proteins have a turnover velocity of between 50 and many thousands of cycles per second, much larger than the frequencies observed here. Still, somehow the cotransporters of interest appear to be most active only during limited times. We speculate that these cotransporters are activated all across the cells by some unspecified signal with the periodicity noted. There is evidence that several molecular signals (ATP, Ca^{2+}, cyclic AMP) act as agonists for endothelial fluid transport [11], and that some (Ca^{2+} waves) are cyclic [12]. Still, the elucidation of the periodicity noted may arise from other mechanisms, and will require further experimental work. Further implications are that neither the number of cotransporters nor the number of charges transported varies much in each cycle.

A. The electrogenic sodium bicarbonate transporter

There is electrophysiological evidence for sodium bicarbonate cotransport in the corneal endothelium. The existence of a symport that transports sodium and bicarbonate out of the cell at the apical membrane in this preparation is strongly supported by the electrophysiological evidence of the Wiederholt laboratory [13–17]. Immunocytochemical localization found cotransporters in both the basolateral and apical membranes [18].

As a result of the operation of the sodium bicarbonate cotransporters in tandem, bicarbonate enters the cell basolaterally, and exits apically [18]. In fact, experimental measurements of a net flux of bicarbonate in this direction have been reported [18,19]. This flux (together with other ionic movements across the cell) generates a transtissue electrical potential difference [20] (aqueous negative). As the cells are separated from each other by relatively leaky junctional complexes [21] which are endowed with negative fixed electrical charges [22], this transtissue electrical field would result in a stream of positive charges (Na^+ ions) through the junction. Such a stream is suggested by the measurement of a net flow of radioactive sodium across the endothelium that stops in the absence of a transtissue electric field [3]. This far, the experimental determination of ionic fluxes is a tangible reality, which poses the question of the nature of the coupling to water movements. Simple osmosis does not appear likely, as there is residual fluid flow in the absence of net solute transport [23]. On the other hand, there are indications that such coupling would be electro-osmotic [24,25]. Further experimentation is required to answer this question.

ACKNOWLEDGMENTS

This work was supported by CONICET PIP No. 1688 (to J.F.). N.M. was a doctoral fellow (CONICET).

[1] D. M. Maurice, in *The Eye*, edited by H. Davson (Academic Press, Orlando, FL, 1984), Vol. 1b, p. 1.
[2] P. Barfort and D. M. Maurice, Exp. Eye Res. **19**, 11 (1974).
[3] S. Hodson, J. Physiol. **236**, 271 (1974).
[4] N. Montalbetti and J. Fischbarg, Biophys. J. **97**, 1530 (2009).
[5] J. Fischbarg and J. J. Lim, J. Physiol. **241**, 647 (1974).
[6] J. J. Lim and J. Fischbarg, Biophys. J. **36**, 677 (1981).
[7] S. Dikstein and D. M. Maurice, J. Physiol. **221**, 29 (1972).
[8] *Wavelets in Medicine and Biology*, edited by M. Aldroubi and M. A. Unser (CRC Press, Boca Raton, FL, 1996).
[9] P. S. Addison, *The Illustrated Wavelet Transform Handbook*. (Institute of Physics Publishing, London, 2002).
[10] J. G. Proakis and D. K. Manolakis, *Digital Signal Processing*, 4th ed. (Prentice-Hall, Saddle River, NJ, 2006).
[11] J. A. Bonanno, Prog. Retinal Eye Res. **22**, 69 (2003).
[12] P. Gomes, S. P. Srinivas, J. Vereecke, and B. Himpens, Exp. Eye Res. **83**, 1225 (2006).
[13] M. Wiederholt, T. J. Jentsch, and S. K. Keller, Pflugers Arch. **405** Suppl. 1, S167 (1985).
[14] T. J. Jentsch, S. K. Keller, M. Koch, and M. Wiederholt, J. Membr. Biol. **81**, 189 (1984).

[15] T. J. Jentsch, H. Matthes, S. K. Keller, and M. Wiederholt, Pflugers Arch. **403**, 175 (1985).
[16] T. J. Jentsch, P. Schwartz, B. S. Schill, B. Langner, A. P. Lepple, S. K. Keller, and M. Wiederholt, J. Biol. Chem. **261**, 10673 (1986).
[17] T. J. Jentsch, T. R. Stahlknecht, H. Hollwede, D. G. Fischer, S. K. Keller, and M. Wiederholt, J. Biol. Chem. **260**, 795 (1985).
[18] F. P. Diecke, Q. Wen, J. Kong, K. Kuang, and J. Fischbarg, Am. J. Physiol. **286**, C1434 (2004).
[19] S. Hodson and F. Miller, J. Physiol. **263**, 563 (1976).
[20] J. Fischbarg, Biochim. Biophys. Acta **228**, 362 (1972).
[21] J. Fischbarg, Exp. Eye Res. **15**, 615 (1973).
[22] J. J. Lim, L. S. Liebovitch, and J. Fischbarg, J. Membr. Biol. **73**, 95 (1983).
[23] F. P. Diecke, L. Ma, P. Iserovich, and J. Fischbarg, Biochim. Biophys. Acta **1768**, 2043 (2007).
[24] A. Lyslo, S. Kvernes, K. Garlid, and S. K. Ratkje, Acta Ophthalmol. **63**, 116 (1985).
[25] J. M. Sanchez *et al*., J. Membr. Biol. **187**, 37 (2002).